Res Chem Intermed
https://doi.org/10.1007/s11164-018-3262-y

Multispectroscopic and theoretical studies on rapid, selective and sensitive visual sensing of cyanide ion in aqueous solution by receptors possessing varying HBD property

P. Raja Lakshmi[1] · R. Manivannan[1] · P. Jayasudha[1] · Kuppanagounder P. Elango[1]

Received: 24 September 2017 / Accepted: 8 January 2018

Abstract Three new benzoquinone–imidazole ensembles possessing varying number (0, 1 and 2) of electron-withdrawing bromo substituents on the quinone ring have been designed, synthesized, characterized and employed as receptors in cyanide sensing. These receptors colorimetrically sense cyanide ion selectively and sensitively in aq. 4-(2-hydroxyethyl)-1-piperazineethanesulphonic acid (HEPES) buffer–acetonitrile (ACN) (8:2 v/v) medium with striking colour change that can easily be seen visually. Fluorescence spectral studies revealed that the receptors form strong complex at 1:1 stoichiometry with cyanide ion. The binding constants for the complexes were found to be in the order of 10^5–10^7 M^{-1} and increase with increasing number of bromo substituents on the quinone ring. The detection limit of cyanide by these receptors lay in the range of 10^{-8} M. The effects of the number of bromo substituents on the absorption maximum, reduction potential and H-bond donor (HBD) property of imidazole N–H are discussed. The results of spectral studies corroborate well with those of electrochemical and theoretical studies. An easy-to-use test strip was prepared to test cyanide in aqueous solution of sodium cyanide prepared using deep-well water.

Keywords Cyanide · Sensor · Colorimetry · Quinone · H-bonding · Visual detection

Electronic supplementary material The online version of this article (https://doi.org/10.1007/s11164-018-3262-y) contains supplementary material, which is available to authorized users.

✉ Kuppanagounder P. Elango
drkpelango@rediffmail.com

[1] Department of Chemistry, Gandhigram Rural Institute (Deemed to be University), Gandhigram 624302, India

Published online: 22 January 2018

Introduction

Cyanide ion is extremely toxic to mammals because it binds strongly to the active sites of cytochrome c oxidase even at very low concentrations, thereby inhibiting the mitochondrial electron transport chain, leading to vomiting, loss of consciousness and ultimately death [1–3]. On the other hand, cyanide is used in many industrial processes, like electroplating, gold mining, chemical processing etc. [4–8]. According to the World Health Organization (WHO), the permissible limit of cyanide ion in drinking water is 1.9 μM [9, 10]. Therefore, selective and sensitive detection of cyanide in water has attracted considerable attention recently. Although a variety of sensors that work via different mechanisms have been documented [11], it is essential to develop feasible and efficient colorimetric sensors for cyanide detection in aqueous solution under mild conditions. Among the various chemical sensors, colorimetric chemosensors have attracted more attention due to benefits including visual detection, operational simplicity, low cost and high sensitivity.

We recently designed quinone-based receptors for selective cyanide sensing, demonstrating that naphthoquinone–imidazole ensemble (**II**) can sense cyanide and fluoride ions colorimetrically in dimethylsulphoxide (DMSO), with the H-atom (N–H) being relatively more acidic (compared with benzimidazole, **I**) when directly attached to quinone as a result of enhanced intramolecular charge-transfer (ICT) transition [12]. Such an acidic H-atom would behave as a relatively better H-bond donor towards the anion, and **II** exhibited cyanide ion binding constant of $5.9 \times 10^3\ M^{-1}$ in DMSO.

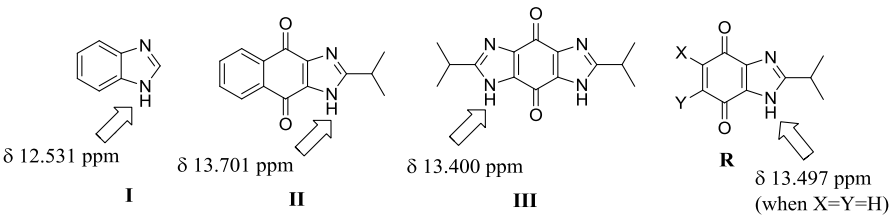

Later, on the basis that receptors with greater number of binding sites would show selectivity and also could accommodate a greater amount of water from the sensing medium, we designed **III**, which contains imidazole on either side of the quinone ring but still possesses a relatively more acidic H-atom (than **I**). We found that **III** binds strongly to cyanide ion selectively in aq. HEPES buffer–dimethylformamide (DMF) (9:1 v/v) medium with binding constant of $1 \times 10^6\ M^{-1}$ [13]. Having shown the satisfactory design and performance of **III** in aqueous medium, it was presumed that a structurally similar receptor (**R**) containing imidazole ring on one side of the quinone ring but leaving the other side free for a substituent of our choice would also exhibit parallel cyanide ion sensing behaviour. Also, introduction of electron-withdrawing substituents at X and Y positions could further enhance the acidity of the imidazole H-atom and hence its HBD property towards the anion. With this intention, in the present study, we designed, synthesized and screened the

anion sensing behaviour of three receptors (**R1**: X = Y = H; **R2**: X = Br, Y = H; **R3**: X = Y = Br). Interestingly these receptors colorimetrically sense cyanide ion selectively in aqueous solution, and increase in the number of bromo substituents enhanced the HBD property of the H-atom towards cyanide ion. Though many receptors, wherein benzimidazole moiety acts as the anion binding unit, have been reported in literature [14–17], the present receptor molecules were designed to have enhanced HBD property toward the analyte as described above.

Therefore, the main objectives of the present endeavour are synthesis, characterization and investigation of the anion sensing behaviour of these three new benzoquinone–imidazole ensembles (**R1**–**R3**). The receptors were characterized using ^{1}H and ^{13}C nuclear magnetic resonance (NMR), mass and Fourier-transform infrared (FTIR) spectral techniques. The cyanide ion sensing properties of these receptors were explored using ultraviolet–visible (UV–Vis), fluorescence and NMR spectral studies. Electrochemical and theoretical studies were also carried out to provide further insight into the mechanism of the sensing process. The effect of increasing the number of bromo substituents on the HBD property of these receptors is also discussed.

Experimental

Chemicals and apparatus

All reagents for synthesis of the receptors were obtained commercially and used without further purification. Spectroscopic-grade solvents were used as received. Double-distilled water was used throughout the work, with the second distillation carried out using alkaline permanganate. UV–Vis spectral studies were carried out using a double-beam spectrophotometer. Steady-state fluorescence spectra were obtained using a spectrofluorimeter. The excitation and emission slit width (5 nm) and scan rate (250 mV s^{-1}) were kept constant for all experiments. Nuclear magnetic resonance spectra were recorded in DMSO-d_6 (600 MHz). ^{1}H NMR spectral data are expressed in the form: chemical shift in units of ppm (normalized integration, multiplicity, and value of *J* in Hz). Electrospray ion mass spectra (*m*/*z*) were recorded using an LC/MSD TRAP XCT Plus (1200 Agilent). Differential pulse voltammetric (DPV) experiments using 1 mmol solutions of the compounds were carried out using glassy carbon (GC) working electrode, Pt wire reference electrode, and Ag wire auxiliary electrode in acetonitrile containing 0.1 M tetrabutylammonium perchlorate as supporting electrolyte at scan rate of 100 mV s^{-1}.

Synthesis and characterization of intermediates

Synthesis of intermediates **1** and **2**: Intermediates 1,2-dinitro-3,6-dimethoxybenzene (**1**) and 1,2-diamino-3,6-dimethoxybenzene (**2**) were prepared from commercially available 1,4-dimethoxybenzene as reported earlier [18, 19] (Scheme 1). Intermediate **2** was characterized using ^{1}H and ^{13}C NMR and LC–MS spectral techniques:

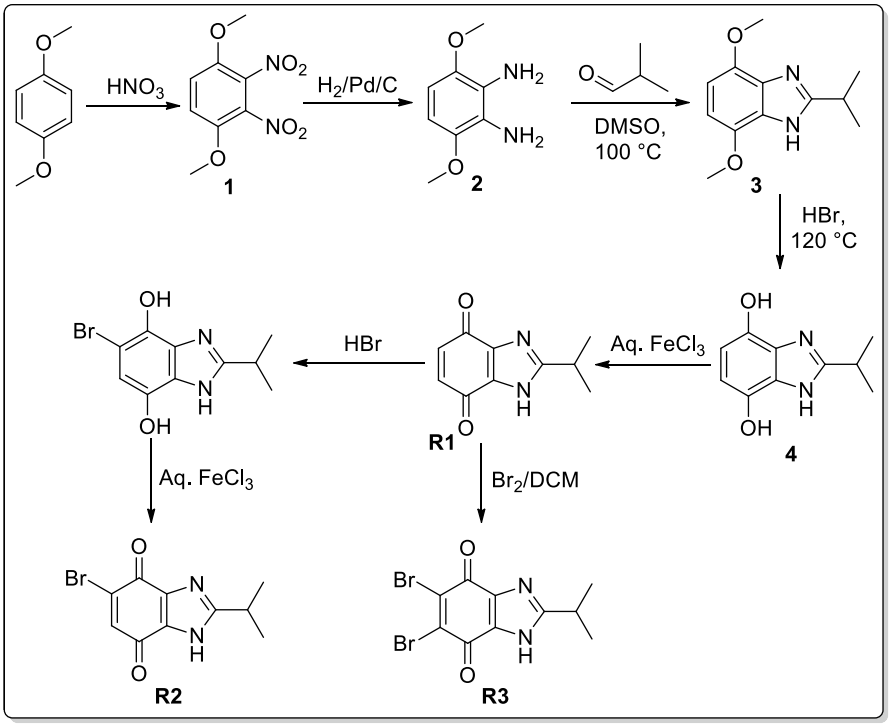

Scheme 1 Synthesis of receptors **R1**–**R3**

Brown solid (3.36 g, yield 91%); δ_H (600 MHz; DMSO-d_6; Me_4Si/ppm): 3.67 (6H, s), 4.10 (4H, s), 6.15 (2H, s), (Fig. S1). δ_C (150 MHz; DMSO-d_6; Me_4Si): 56.16, 99.85, 124.42, 142.58 (Fig. S2). LC–MS (ESI-APCI) *m/z*: cacld. for $C_8H_{12}N_2O_2$, 168.19, found, 169.20 $[M + H]^+$ (Fig. S3).

Synthesis of intermediate **3**: Intermediate **3** was prepared using the procedure for preparation of similar compounds reported earlier [12]. A mixture of **2** and isobutyraldehyde (1 eqv.) in DMSO (5 mL) was heated at 100 °C with stirring for 6 h. After cooling to room temperature, the precipitate obtained from the reaction mixture was filtered through filter paper and washed with cold ethanol to obtain pure product 2-isopropyl-4,7-dimethoxybenzimidazole (**3**). Intermediate **3** was characterized using ^1H and ^{13}C NMR and LC–MS spectral techniques: White solid (3 g, yield 77%); δ_H (600 MHz; DMSO-d_6; Me_4Si/ppm): 1.30–1.31 (6H, d, $J = 6.6$ Hz), 3.07–3.11 (1H, m), 3.84–3.85 (6H, d, $J = 5.4$ Hz), 6.53 (2H, s), 12.27 (1H, s) (Fig. S4). δ_C (150 MHz; DMSO-d_6; Me_4Si): 21.95, 28.71, 56.04, 102.51, 134.57, 141.42, 158.71 (Fig. S5). LC–MS (ESI-APCI) *m/z*: cacld. for $C_{12}H_{16}N_2O_2$, 220.27, found, 221.30 $[M + H]^+$ (Fig. S6).

Synthesis of intermediate **4**: Intermediate 2-isopropyl-4,7-dimethoxy benzimidazole (**3**) was refluxed with 48% hydrobromic acid (3 eqv.) for 6 h. The reaction mixture was cooled and extracted using ethyl acetate and water to yield crude

2-isopropyl-4,7-dihydroxybenzimidazole (**4**), which was used without further purification [18, 19].

Synthesis of receptor R1 (2-isopropyl-1*H*-benzo[*d*]imidazole-4,7-dione)

2-Isopropyl-4,7-dihydroxybenzimidazole (intermediate **4**) was treated with 2 eqv. ferric chloride dissolved in 10 mL water and stirred at RT for 3 h. After reaction completion, the reaction mixture was partitioned with ethyl acetate. The organic layer was concentrated and dried using sodium sulphate, then purified by column chromatography to yield the pure product. The receptor was characterized using ^{1}H and ^{13}C NMR and LC–MS spectral techniques: Yellow solid (2.1 g, yield 81%). δ_H (600 MHz; DMSO-d_6; Me_4Si): 1.27–1.29 (d, 6H, J = 7.2 Hz), 3.05–3.09 (m, 1H), 6.67 (s, 2H), 13.49 (s, 1H) (Fig. S7); δ_C (150 MHz; DMSO-d_6; Me_4Si): 21.55, 28.44, 132.64, 135.91, 136.86, 140.87, 160.27, 178.19, 181.75 (Fig. S8). LC–MS (ESI-APCI) *m*/*z*: Calcd. for $C_{10}H_{10}N_2O_2$: 190.20; Found: 191.20 $[M + H]^+$ (Fig. S9).

Synthesis of receptor R2 (5-bromo-2-isopropyl-1*H*-benzo[*d*] imidazole-4,7-dione)

Compound **R1** was treated with 48% hydrobromic acid (2 eqv.) and refluxed for 6 h. The reaction mixture was cooled and extracted using ethyl acetate and water to yield crude 5(6)-bromo-4,7-dihydroxy-2-isopropylbenzimidazole, which was used without further purification. The obtained crude was treated with 2 eqv. ferric chloride dissolved in 10 mL water and stirred at RT for 3 h. The reaction mixture was extracted with ethyl acetate and dried using sodium sulphate, then purified by column chromatography. The receptor was characterized using ^{1}H and ^{13}C NMR and LC–MS spectral techniques: Orange solid (151 mg, yield 53%); δ_H (600 MHz; DMSO-d_6; Me_4Si): 1.27–1.29 (d, 6H, J = 7.2 Hz), 3.05–3.10 (m, 1H), 7.31 (s, 1H), 13.71 (s, 1H) (Fig. S10). δ_C (150 MHz; DMSO-d_6; Me_4Si): 21.51, 28.48, 133.02, 137.30, 139.16, 142.05, 160.99, 179.14, 182.37 (Fig. S11). LC–MS (ESI-APCI) *m*/*z*: Calcd. for $C_{10}H_9BrN_2O_2$: 269.09; Found: 270.20 $[M + H]^+$ (Fig. S12).

Synthesis of receptor R3 (5,6-dibromo-2-isopropyl-1*H*-benzo[*d*] imidazole-4,7-dione)

Compound **R1** was dissolved in dichloromethane (5 mL), cooled to 0 °C, then bromine (2 eqv.) was added dropwise and stirred at RT for 2 h. The reaction mixture was extracted with ethyl acetate and water, then purified by column chromatography to yield the pure product. The receptor was characterized using ^{1}H and ^{13}C NMR and LC–MS spectral techniques: Orange solid (138 mg, yield 50%). δ_H (600 MHz; DMSO-d_6; Me_4Si): 1.28–1.29 (d, 6H, J = 7.2 Hz), 3.06–3.10 (m, 1H), 13.79 (s, 1H) (Fig. S13); δ_C (150 MHz; DMSO-d_6; Me_4Si): 21.49, 28.47, 128.06, 129.31, 132.27, 139.16, 161.24, 181.35, 183.12 (Fig. S14); LC–MS (ESI-APCI) *m*/*z*: Calcd. for $C_{10}H_8Br_2N_2O_2$: 347.99; Found: 349.30 $[M + H]^+$ (Fig. S15).

Results and discussion

The three new receptors (**R1**–**R3**) were prepared from commercially available starting materials as depicted in Scheme 1. The receptors were characterized using ^{1}H and ^{13}C NMR, FTIR and mass spectral techniques. The FTIR spectrum of free **R1** exhibited an intense single peak at 1665 cm^{-1} corresponding ν(C=O) of quinone ring (Fig. 1). In the case of free **R3** (Fig. S16–S18), this peak appeared at 1679 cm^{-1}, also as a single peak. However, in the case of free **R2**, the peak due to quinone carbonyl stretching underwent splitting and appeared at 1683 and 1647 cm^{-1}; That is, in receptors **R1** and **R3**, both carbonyl groups are nearly similar and their lengths equal. This may be due to the presence of symmetrical substituents at X and Y positions in **R1** (both H) and **R3** (both Br) and unsymmetrical substitution in **R2** (H and Br). Further, the shift in this stretching frequency from 1665 to 1679 cm^{-1} from **R1** to **R3** suggests that, as the number of bromo substituents was increased, the electron-withdrawing power of the quinone moiety increased, shortening the carbonyl bond [20]. The anion-sensing properties of these receptors were investigated using spectral, electrochemical and theoretical studies.

Visual detection

As a preliminary investigation, the change in colour of these receptors in absence and presence of various anions such as F^-, Cl^-, Br^-, CN^-, $H_2PO_4^-$, OAC^-, I^-, NO_3^-, NO_2^-, S^{2-} and NCS^- was observed visually in aq. HEPES buffer–ACN (8:2 v/v) medium. The results obtained are shown in Figs. 2 and S19. It is evident from these figures that these receptors instantaneously changed their colour only

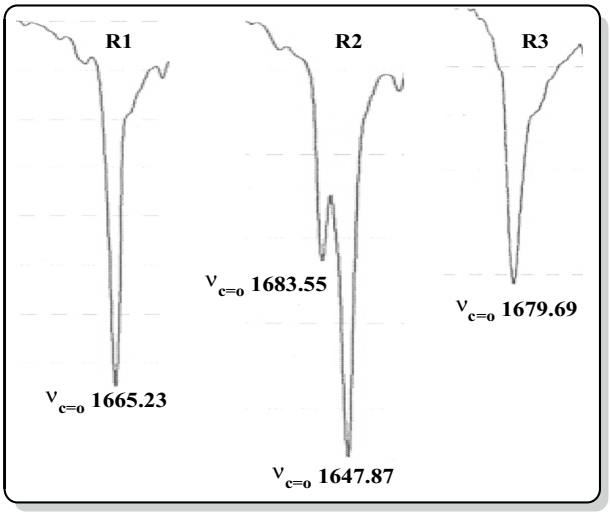

Fig. 1 Partial FTIR spectra of receptors, showing carbonyl stretching peak

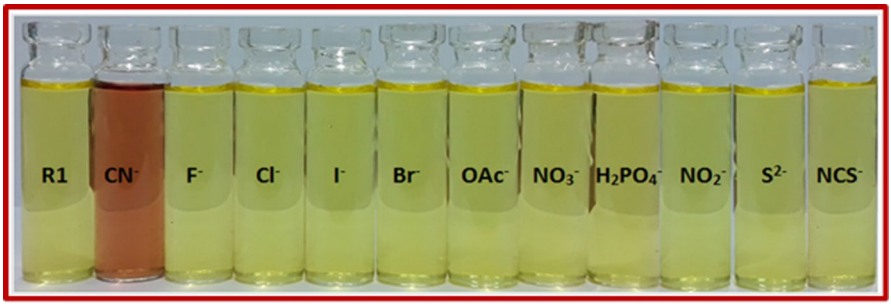

Fig. 2 Colour changes observed in aq. HEPES buffer–ACN (8:2 v/v) solution of **R1** (7.5×10^{-4} M) upon addition of one equivalent of various anions

in presence of cyanide ion; with all other chosen anions, no observable change in colour was noticed. This indicates the selectivity of the receptors toward cyanide ion. The change in colour of receptor **R1**, as a representative case, with addition of one equivalent of common metal ions is also shown in Fig. S20. As seen from this figure, the colour of the receptor remained unchanged upon addition of the chosen metal ions, confirming the selectivity of the receptors towards cyanide ion. As a representative case, the change in colour of **R1** in absence and presence of cyanide at different pH values is collected in Fig. S21. The results indicate that the receptor can sense cyanide in neutral medium. The results of these visual detection experiment are well supported by the electronic spectral data (Fig. S22). The change in colour of the receptor itself in basic medium suggested that the mechanism of sensing may involve H-bond formation between N and H moiety and cyanide ion, as hydroxide ion is a well-known deprotonating agent [21].

Electronic spectral studies

The electronic spectra of 7.5×10^{-6} M solution of these receptors in aq. HEPES–ACN (8:2 v/v) showed a band at 399 (log ε 4.68), 417 (log ε 4.67) and 426 nm (log ε 4.59) for **R1**, **R2**, and **R3**, respectively (Figs. 3, S23, S24). This absorption band corresponds to the characteristic intramolecular charge-transfer (ICT) transition from imidazole nitrogen atoms to the electron-deficient quinone ring [12]. It is seen that, as the number of electron-withdrawing bromo substituents increased from **R1** to **R3**, the ICT transition was found to occur energetically more easily, as expected. This observation corroborates the FTIR spectral results. Furthermore, as the ICT transition becomes easier, the H-atom (N–H) will become more acidic and thus act as a relatively better H-bond donor towards cyanide ion. The selectivity towards cyanide ion of these receptors was further confirmed by electronic spectral studies in absence and presence of one equivalent of chosen anions such as F^-, Cl^-, Br^-, CN^-, $H_2PO_4^-$, OAC^-, I^-, NO_3^-, NO_2^-, S^{2-} and NCS^-. It is evident from Fig. S25 that the ICT transition band of **R1** (as a representative case) at 399 nm exhibited a red-shift only in presence of cyanide ion, confirming the selectivity of these receptors towards cyanide.

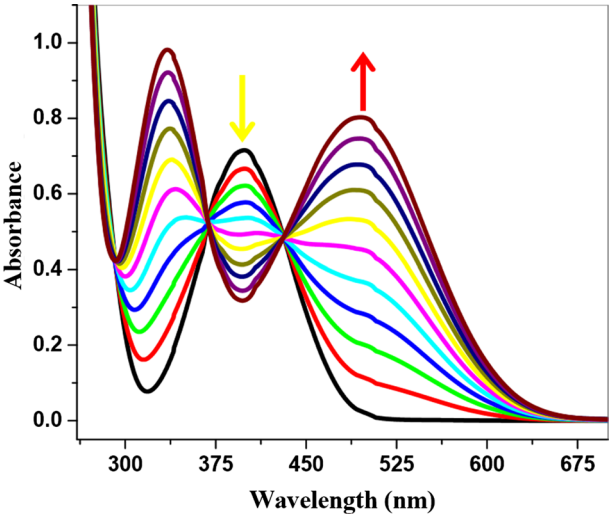

Fig. 3 UV–Vis spectra of **R1** (7.5×10^{-6} M) with incremental addition of cyanide (0–7.5×10^{-6} M) in aq. HEPES buffer–ACN (8:2 v/v) medium

The nature of the binding between the receptors and cyanide ion was investigated using electronic spectral titration studies (Figs. 3, S23, S24). It is evident from these figures that, upon addition of incremental amounts of cyanide to solution of these receptors, the absorbance of the ICT transition band decreased gradually with concomitant increase in the absorbance of a new band at relatively higher wavelength. Such electronic spectral behavior suggests that addition of cyanide makes the ICT transition energetically easier. This may be due to formation of H-bond between imidazole N–H group and cyanide ion. Such a H-bond would increase the electron density on the N-atom (N–H) and thus make the ICT transition energetically easier [21]. The red-shifts observed in λ_{ICT} were found to be 96, 90 and 97 nm for **R1**, **R2** and **R3**, respectively. Such a large shift ($\Delta\lambda_{ICT}$) indicates strong interaction between the receptors and cyanide ion. Furthermore, the appearance of a clear isosbestic point (at 431, 445 and 448 nm for **R1**, **R2** and **R3**, respectively) suggests presence of two species in equilibrium in the solution, viz. free receptor (N–H) and H-bonded receptor (N–H…CN^-) [12]. The stoichiometry of the receptor–CN^- complexes was determined by Job's continuous variation method (Fig. S26) [22]. In all the three cases, Job's curve showed a maximum at mole fraction of 0.5, indicating 1:1 stoichiometry.

Fluorescence spectral studies

The intensity of binding between the receptors and cyanide ion was assessed by fluorescence spectral titration studies. The fluorescence spectra of the receptors with addition of incremental amounts of cyanide are shown in Figs. 4, S27 and S28. As seen from these spectra, the free receptors showed strong emission ($\lambda_{ex}/\lambda_{em}$ at

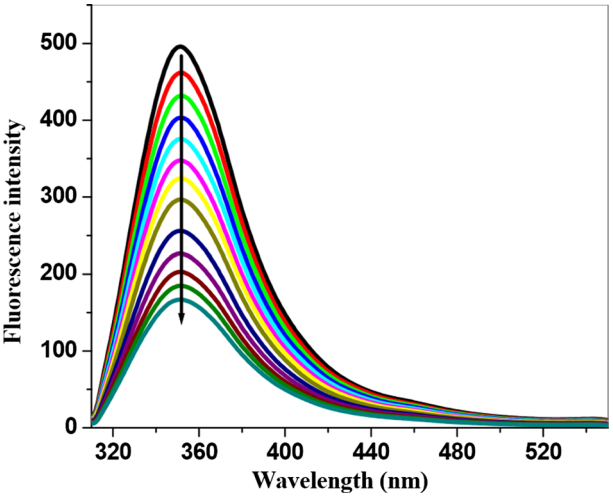

Fig. 4 Fluorescence spectra of **R1** (7.5×10^{-5} M) with incremental addition of cyanide ($0–7.5 \times 10^{-5}$ M) in aq. HEPES buffer–ACN (8:2 v/v) medium

302/351, 330/426 and 330/428 nm for **R1**, **R2** and **R3**, respectively), which was quenched upon addition of cyanide ion, indicating formation of a complex between them (receptor–CN^- complex). The binding constants of the complexes were determined from the fluorescence spectral data using the Benesi–Hildeband equation [23]. The plots for these receptors were found to be linear ($r > 0.99$). The binding constants were found to be 5.6×10^5, 1.5×10^6 and 5.2×10^7 M^{-1} for **R1**, **R2** and **R3**, respectively. The magnitude of the binding constant indicates formation of strong receptor–CN^- complexes in the present study. The steady increase in the binding constant value from **R1** to **R3** is due to the fact that increasing the number of electron-withdrawing bromo substituents on the quinone ring increased the intensity of the ICT transition and thus the acidity (HBD property) of the H-atom (N–H), strengthening its binding with cyanide ion.

The fluorescence quenching in these receptors caused by cyanide ion was quantified by measuring the quantum yields of the receptors in absence and presence of cyanide ion. The quantum yields, measured using quinine sulphate as standard [24], were found to be 0.525, 0.647 and 0.789 for free receptor **R1**, **R2** and **R3**, respectively. The quantum yields for the receptor–CN^- complexes, after addition of one equivalent of cyanide, were observed to be 0.346, 0.409 and 0.412, respectively (Fig. S29–S35). This reduction in the quantum yield values in the receptor–CN^- complexes compared with corresponding free receptors strongly supports the quenching of fluorescence of the receptors by cyanide through complex formation. The detection limits, at $S/N = 3$, of cyanide by these receptors were computed as reported elsewhere [25–28]. The results thus obtained were 64×10^{-8}, 8×10^{-8} and 5×10^{-8} M for **R1**, **R2** and **R3**, respectively (Fig. S36–S38). The observed limits of detection of cyanide using these receptors are far below the level recommended by WHO (1.9×10^{-6} M).

NMR spectral studies

To delineate the mechanism of interaction of cyanide with the receptors, ^{1}H NMR spectral titration studies were carried out in DMSO-d_6. The spectra obtained in absence and presence of various amounts of cyanide are depicted in Figs. 5, S39, S40. The signal corresponding to N–H proton in **R1** appeared at 13.497 ppm, higher than in simple benzimidazole (12.531 ppm). This is due to the fact that, when imidazole N–H is directly attached to electron-deficient quinone ring, due to the existence of ICT transition, the N–H proton becomes more acidic. This signal (δ_{NH}) in **R2** and **R3** appeared at 13.708 and 13.787 ppm, respectively. It is evident from these spectra that increasing the number of bromo substituents progressively increased the acidity of the N–H proton and hence its HBD property. This is in line with our perception spelt out in "Introduction" section.

As seen from Fig. 5, upon addition of 0.5 equivalent cyanide to the solution of **R1**, the signal due to N–H proton was found to be deshielded from 13.497 to 13.553 ppm with broadening. Furthermore, this signal was found to disappear after addition of one equivalent of cyanide. The other two receptors showed similar spectral behaviour on addition of cyanide (Fig. S39, S40). These observations indicate that the cyanide sensing mechanism of these receptors involves formation of H-bond between N–H and cyanide ion followed by deprotonation (Scheme 2) [12]. This proposed mechanism accounts for the results obtained in the electronic and fluorescence spectral studies. The observed increase in the binding constants of the receptor–CN^- complexes, from **R1** to **R3**, is due to the increase in the HBD property of the N–H group with increase in the number of bromo substituents in these receptors.

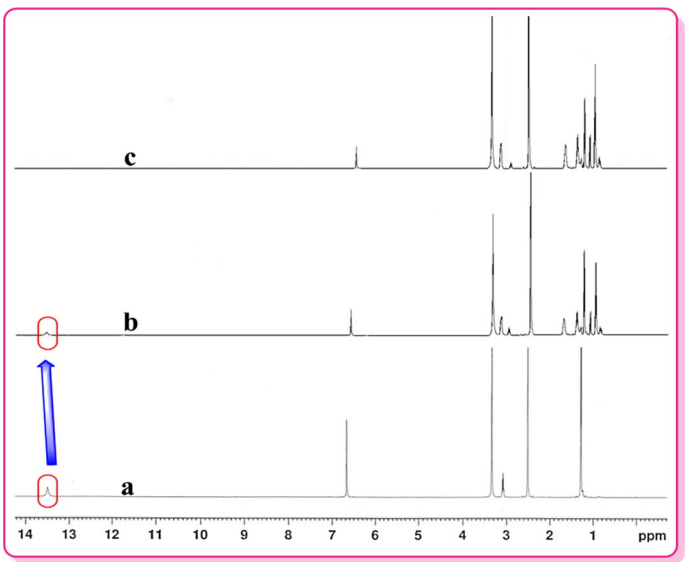

Fig. 5 ^{1}H NMR spectrum of **R1** with addition of **a** 0 eqv., **b** 0.5 eqv., and **c** 1.0 eqv. cyanide in DMSO-d_6

Scheme 2 Cyanide ion sensing mechanism of receptors

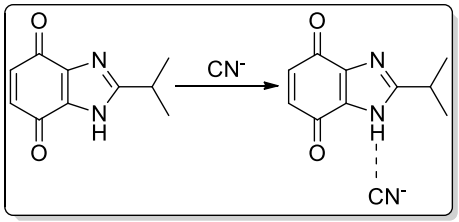

The N-atom (of N–H group), after deprotonation, becomes relatively electron rich, which makes the ICT transition from such a N-atom to quinone energetically easier, hence the receptor–CN^- complex absorbs at higher wavelength [13].

Electrochemical studies

To support the observations made in spectral studies, regarding the effect of increasing the number of bromo substituents on the behaviour of the receptors, electrochemical study was also carried out. The differential pulse voltammograms of the receptors recorded in ACN with tetrabutylammonium perchlorate as supporting electrolyte are shown in Figs. 6, S41, S42. The voltammogram for electroreduction of quinone ring showed two characteristic reduction peaks (at E_{pc} = **R1**: − 0.512, −0.864; **R2**: − 0.484, − 0.840; **R3**: − 0.444, − 0.796 V). The first peak at lower negative potential is due to formation of radical anion ($Q^{\cdot-}$), while the second peak at relatively higher negative potential corresponds to formation of dianion (Q^{2-}) [29]. Furthermore, the reduction potential of both peaks decreased from **R1** to **R3**,

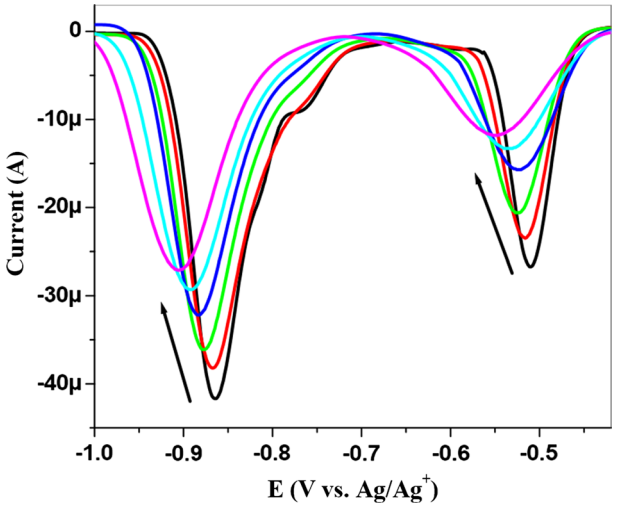

Fig. 6 Changes in redox properties of **R1** upon addition of cyanide in acetonitrile

making electroreduction of the quinone easier, due to increase in the number of electron-withdrawing bromo substituents. It is evident from these voltammograms that, upon addition of incremental amounts of cyanide ion to the receptor solution, both reduction peaks shifted to higher negative potential with a concurrent decrease in current density. This shift to relatively higher potential suggests that electroreduction of the quinone becomes difficult upon addition of cyanide ion. This is due to the fact that addition of cyanide ion makes the ICT transition easier and thus increased the electron density on the quinone ring, making electroreduction difficult [13, 21].

Theoretical studies

Density functional theory calculations at B3LYP/3-21G basis level set were carried out using the Gaussian 03 package to estimate the electronic properties of these receptors before and after addition of cyanide ion [30]. The optimized geometries and the orientation of the highest occupied molecular orbital (HOMO) and lowest unoccupied molecular orbital (LUMO) in the free receptors and their receptor–CN^- complexes are shown in Figs. S43, S44, S45. The energies of the MOs are collected in Table S1. In the free receptors, the HOMO was localized on the imidazole ring and the LUMO concentrated on the quinone moiety. Such a MO distribution is a prerequisite for a compound to be an ICT probe [31]. The energy corresponding to the ICT transition (ΔE) is the difference in energy between these MOs. The results in Table S1 show that the ΔE values were relatively lower in the receptor–CN^- complex than in the corresponding free receptor, indicating an energetically easier ICT transition in the complex. Thus, the results of this theoretical study are in good agreement with the red-shifts observed in the electronic spectra of the receptors after addition of cyanide ion.

Practical application

Since these receptors colorimetrically sense cyanide with a striking colour change in aqueous solution, easy-to-use inexpensive test strips were prepared by immersing filter paper into solution of **R1** (as a representative case) and drying in air (Fig. 7). Sodium cyanide solutions of various concentrations were prepared using deep-well water. The composition of the deep-well water employed in the present study is (all in mg/L except pH): pH 8.02, total alkalinity 358, total hardness 271, total dissolved solids 1403, Cl^- 198, F^- 1.02, SO_4^{2-} 46. As seen from the figure, when the test strips were immersed in variation concentrations of cyanide in water, the colour of the strips immediately changed, being easily seen visually. Therefore, the prepared strips are an effective test-kit for detection of cyanide ion in water with high selectivity for use in real-time applications.

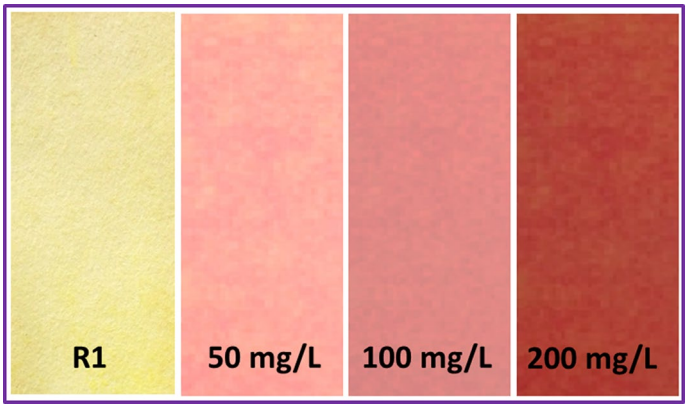

Fig. 7 Colour change of test strips upon dipping in cyanide ion solution in water

Conclusions

Three new benzoquinone–imidazole ensembles containing varying numbers of bromo substituents were designed, synthesized and characterized. These receptors colorimetrically sense cyanide ion selectively and sensitively in aqueous solution. Increasing the number of bromo substituents on the quinone ring had a marked influence on the spectral, electrochemical and cyanide ion binding properties of the receptors, as shown below:

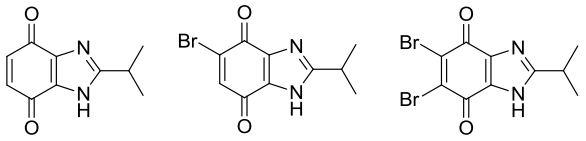

	R1	R2	R3
λ_{ICT} (nm)	399	417	426
δ_{NH} (ppm)	13.497	13.708	13.787
E_{pc} (V)	-0.512, -0.864	-0484, -0.840	-0.444, -0.796
K (M^{-1})	$5.6x10^5$	$1.5x10^6$	$5.2x10^7$

The cyanide sensing mechanism of these receptors involves formation of H-bond between imidazole N–H group and cyanide ion. The detection limit of cyanide by the receptors was in the order of 10^{-8} M, much lower than the permissible limit of cyanide ion in drinking water set by the WHO (1.9×10^{-6} M). Electrochemical and theoretical studies were carried out to substantiate the proposed sensing mechanism. Easy-to-use test strips were developed as a useful cyanide test-kit for

field measurements. It is interesting to compare the results of the present study with those for structurally analogous quinone–imidazole ensembles **II** and **III**. Receptors **R1**–**R3** sensed cyanide selectively in aqueous solution, similar to **III**, while **II** exhibited colour change with both cyanide and fluoride in DMSO. The novelty of the present receptors is that one can tune the HBD property by varying the number of bromo substituents on the quinone ring, which is possible with the present structural design, in contrast to **III**.

References

1. Q. Li, J.H. Zhang, Y. Cai, W.J. Qu, G.Y. Gao, Q. Lin, H. Yao, Y.M. Zhang, T.B. Wei, Tetrahedron **71**, 857 (2015)
2. V. Amendola, D.E. Gomez, L. Fabbrizzi, M. Licchelli, Acc. Chem. Res. **39**, 343 (2006)
3. C. Suksai, T. Tuntulani, Chem. Soc. Rev. **32**, 192 (2003)
4. T.Z. Sadyrbaeva, Sep. Purif. Technol. **86**, 262 (2012)
5. V.K. Sharma, C.R. Burnett, R.A. Yngard, D.E. Cabelli, Environ. Sci. Technol. **39**, 3849 (2005)
6. K. Naicker, E. Cukrowska, T.S. McCarthy, Environ. Pollut. **122**, 29 (2003)
7. Y.C. Yang, J.A. Barker, J.R. Ward, Chem. Rev. **92**, 1729 (1992)
8. G.Q. Liu, W.T. Yen, Miner. Eng. **8**, 111 (1995)
9. Q. Lin, Y. Cai, Q. Li, B.B. Shi, H. Yao, Y.M. Zhang, T.B. Wei, Spectrochim. Acta A **141**, 113 (2015)
10. K. Wang, Z. Liu, R. Guan, D. Cao, H. Chen, Y. Shan, Q. Wu, Y. Xu, Spectrochim. Acta A **144**, 235 (2015)
11. F. Huo, J. Kang, C. Yin, J. Chao, Y. Zhang, Sens. Actuators B **215**, 93 (2015)
12. R. Manivannan, A. Satheshkumar, K.P. Elango, New J. Chem. **37**, 3125 (2013)
13. R. Manivannan, S. Ciattini, L. Chelazzi, K.P. Elango, RSC Adv. **5**, 87341 (2015)
14. J.B. Li, J.H. Hu, J.J. Chen, J. Qi, Spectrochim. Acta A **133**, 773 (2014)
15. N. Kumari, S. Jha, S. Bhattacharya, J. Org. Chem. **76**, 8215 (2011)
16. L. Tang, M. Cai, Z. Huang, K. Zhong, S. Hou, Y. Bian, R. Nandhakumar, Sens. Actuators B **185**, 188 (2013)
17. M. Sun, H. Yu, H. Li, H. Xu, D. Huang, S. Wang, Inorg. Chem. **54**, 3766 (2015)
18. P. Hammershoj, T.K. Reenberg, M. Pittelow, C. B. Nielsen, O. Hammerich, J.B. Christensen, Eur. J. Org. Chem. **2006**, 2796 (2006)
19. L. Garuti, M. Roberti, N. Malagoli, P. Rossi, M. Castelli, Bioorg. Med. Chem. Lett. **10**, 2193 (2000)
20. P. Jayasudha, R. Manivannan, S. Ciattini, L. Chelazzi, K.P. Elango, Sens. Actuators B **242**, 736 (2017)
21. P. Jayasudha, R. Manivannan, K.P. Elango, RSC Adv. **6**, 25473 (2016)
22. P. Jayasudha, R. Manivannan, K.P. Elango, Sens. Actuators B **221**, 1441 (2015)
23. J. Ma, Y. Liu, L. Chen, Y. Xie, L.Y. Wang, M.X. Xie, Food Chem. **132**, 663 (2012)
24. Q. Lin, X. Liu, T.B. Wei, Y.M. Zhang, Chem. Asian J. **8**, 3015 (2013)
25. S. Park, K.H. Hong, J.I. Hong, H.J. Kim, Sens. Actuators B **174**, 140 (2012)
26. Y. Yan, H. Yu, K. Zhang, M. Sun, Y. Zhang, X. Wang, S. Wang, Nano Res. **9**, 2088 (2016)
27. Y. Zhang, L. Guan, H. Yu, Y. Yan, L. Du, Y. Liu, M. Sun, D. Huang, S. Wang, Anal. Chem. **88**, 4426 (2016)
28. H. Yu, L. Du, L. Guan, K. Zhang, Y. Li, H. Zhu, M. Sun, S. Wang, Sens. Actuators B **247**, 823 (2017)
29. V.A. Nikitina, R.R. Nazmutdinov, G.A. Tsirlina, J. Phys. Chem. B **115**, 668 (2011)
30. M.J. Frisch, G.W. Trucks, H.B. Schlegel, G.E. Scuseria, M.A. Robb, J.R.Cheeseman, J.A. Montgomery Jr., T. Vreven, K.N. Kudin, J.C. Burant, J.M. Millam, S.S. Iyengar, J. Tomasi, V. Barone, B. Mennucci, M. Cossi, G. Scalmani, N. Rega, G.A. Petersson, H. Nakatsuji, M. Hada, M. Ehara, K. Toyota, R. Fukuda, J. Hasegawa, M. Ishida, T. Nakajima, Y. Honda, O. Kitao, H. Nakai, M. Klene, X. Li, J.E. Knox, H.P. Hratchian, J.B. Cross, V. Bakken, C. Adamo, J. Jaramillo, R. Gomperts, R.E. Stratmann, O. Yazyev, A.J. Austin, R. Cammi, C. Pomelli, J.W. Ochterski, P.Y. Ayala, K. Morokuma, G.A. Voth, P. Salvador, J.J. Dannenberg, V.G. Zakrzewski, S. Dapprich, A.D. Daniels,

M.C. Strain, O. Farkas, D.K. Malick, A.D. Rabuck, K. Raghavachari, J.B. Foresman, J.V. Ortiz, Q. Cui, A.G. Baboul, S. Clifford, J. Cioslowski, B.B. Stefanov, G. Liu, A. Liashenko, P. Piskorz, I. Komaromi, R.L. Martin, D.J. Fox, T. Keith, M.A. Al-Laham, C. Y. Peng, A. Nanayakkara, M. Challacombe, P.M.W. Gill, B. Johnson, W. Chen, M.W. Wong, C. Gonzalez, J.A. Pople, Gaussian 03, Revision D.01, Gaussian, Inc., Wallingford CT (2004)

31. N.M. Ruvalcaba, G. Cuevas, I. Gonzalez, M. Amartinez, J. Org. Chem. **67**, 3673 (2002)